Available online at www.sciencedirect.com
SCIENCE DIRECT®
Journal of Solid State Chemistry 177 (2004) 1338–1345
JOURNAL OF SOLID STATE CHEMISTRY
http://elsevier.com/locate/jssc

Study of magnetransport properties in manganites with fixed structural parameters

E.P. Rivas-Padilla,* P.N. Lisboa-Filho, and W.A. Ortiz

Grupo de Supercondutividade e Magnetismo, Departamento de Física, Centro Multidisciplinar para o Desenvolvimento de Materiais Cerâmicos–CMDMC, Universidade Federal de São Carlos, CP 676 CEP 13565-905, São Carlos, SP, Brazil

Received 30 July 2003; received in revised form 30 October 2003; accepted 6 November 2003

Abstract

This work reports a detailed study of magnetic and transport properties of the manganite compounds $(R1,R2)_{0.67}(M1,M2)_{0.33}MnO_3$ ($R1$, $R2$ = La, Gd, Pr, Tb, Ho; $M1$, $M2$ = Ca, Sr, Ba). Taking into account that the ferromagnetic-to-paramagnetic and the metallic-to-semiconductor transition temperatures, as well as the magnetoresistance peak temperature, depend on the ionic radius of the A-site cations, $\langle r_A \rangle$, as well as on the A-site ($A = R1$, $R2$, $M1$ and $M2$) cationic size mismatch, $\sigma^2(r_A)$, and also on the ratio Mn^{3+}/Mn^{4+}, compositions of the samples employed here were chosen to keep these parameters approximately constant. X-ray diffraction patterns indicate that all samples have similar structural characteristics. Experimental results show that they all present similar ferromagnetic–paramagnetic and metallic–semiconductor transition temperatures, as well as similar behavior of the magnetoresistance. We also found evidences of magnetic coupling between rare-earth and Mn moments at low temperatures, while at high temperatures the rare-earth ions have paramagnetic behavior. These results indicate that by controlling the structural parameters and preparation conditions, one can obtain samples with similar magnetic and electrical properties.
© 2003 Elsevier Inc. All rights reserved.

PACS: 75.47.Lx; 75.47.Gk; 73.43. Qt

Keywords: Magnetoresistance; Manganite; Perovskite

1. Introduction

The discovery of colossal magnetoresistance (CMR) in perovskite-type manganese oxides has generated considerable interest in these materials. These systems, with the general formula $(RE, AE)MnO_3$, where RE is a trivalent rare-earth and AE is a divalent alkali-earth, have being studied not only to understand the basic aspects of the interaction mechanisms present in these compounds, but also for a possible use in technological applications. This situation implies the need to search for materials exhibiting a CMR at room temperature under lower applied magnetic fields. Substitution of the trivalent element by a divalent one produces mixed valence Mn^{3+}/Mn^{4+} affecting both magnetic and transport properties. These properties can be qualitatively described on the basis of the double-exchange (DE) model proposed by Zener [1]. According to this theory, the ferromagnetic interaction between Mn^{3+} and Mn^{4+} is established by the motion of charge carriers in the compounds via oxygen anions. The double-exchange mechanism depends on the Mn–O–Mn bond angle through the matrix element t_{ij}. The decrease in the bond angle reduces t_{ij} which, in turn, governs the electron hopping between Mn sites. This reduction leads to a systematic decrease in the ferromagnetic-to-paramagnetic transition temperature (T_C) [2,3].

Many studies have shown that T_C and the metallic-to-semiconductor transition temperature (T_{MS}), as well as the CMR peak temperature, can be tuned by controlling independently some parameters, as the ionic radius of the A-site cations, $\langle r_A \rangle$, the A-site cationic size mismatch, $\sigma^2(r_A)$, and the relative ratio of manganese atoms with different valences, Mn^{3+}/Mn^{4+} [4,5].

Several authors have reported that T_C and T_{MS} are shifted to higher values with the increase of $\langle r_A \rangle$ and that these temperatures tend to saturate at high $\langle r_A \rangle$

*Corresponding author. Fax: +55-162-608-228.
E-mail address: rivas@df.ufscar.br (E.P. Rivas-Padilla).

0022-4596/$ - see front matter © 2003 Elsevier Inc. All rights reserved.
doi:10.1016/j.jssc.2003.11.007

values, probably because many of these manganites have A-site cations with a large size mismatch [6,7]. Moreover, the disparity of A-site cations, due to the difference in ionic radius, should cause different local distortions of the lattice around rare-earth ions, which could result in magnetic inhomogeneity and lead to complex magnetic structures. To measure the size disparity (or size mismatch effect), Rodriguez-Martinez and Attfield [6,7] employed the statistical variance in the distribution of radii, $\sigma^2(r_A)$. They showed that T_C and T_{MS} in these manganites are very sensitive to the mismatch in the sizes of the A-site cations. They also have found that, keeping $\langle r_A \rangle$ constant for different values of the Mn^{3+}/Mn^{4+} ratio, T_C decreases linearly with $\sigma^2(r_A)$.

These studies indicate the crucial role played by the set of parameters $\langle r_A \rangle$, Mn^{3+}/Mn^{4+} and $\sigma^2(r_A)$, on the electric and magnetic properties but, in most of the cases, the studies were based on materials with only one or two fixed parameters [7,8].

Taking these considerations into account, we have studied the magnetic and transport properties of a number of manganites of the series $(R1_{1-y}R2_y)^{+3}_{0.67}(M1_zM2_{1-z})^{+2}_{0.33}MnO_3$ maintaining all three parameters fixed, i.e., all samples prepared have very similar values of $\langle r_A \rangle$, as well as of Mn^{3+}/Mn^{4+} and $\sigma^2(r_A)$. This situation allows one to predict that the crystallographic structures should be similar and, consequently, so would the Mn–O–Mn bond angles. Therefore, one should expect similar magnetic interactions (double-exchange and superexchange) from one compound to the other. X-ray diffraction and magnetization measurements corroborate those expected results. In this paper we also discuss the role played by rare-earth ions in the A-site, since evidences were found for the occurrence of a coupling between the Mn magnetic structure and the rare-earth moments at low temperatures. The composition with $Mn^{4+} = 0.33$ was chosen because this doping concentration seems to maximize the double-exchange effect, as seen in the lanthanum compounds [9].

2. Experimental procedure

A series of $(R1_yR2_{1-y})^{+3}_{0.67}(M1_zM2_{1-z})^{+2}_{0.33}MnO_3$ ($R1$, $R2$ = La, Gd, Pr, Ho, Tb; $M1$, $M2$ = Ca, Sr) samples were synthesized using a sol–gel method [10]. The samples were prepared with three of the experimental variables, namely $\langle r_A \rangle$, $\sigma^2(r_A)$ and the Mn^{3+}/Mn^{4+} ratio, maintained constant. The stoichiometry of the compounds was calculated using a computational program, specially developed to evaluate all possible combinations of the involved elements ($A = R1$, $R2$, $M1$ and $M2$), with the objective of obtaining the compositions of the samples with the desired parameter values. This series of compounds was prepared with values of $Mn^{4+} = 0.33$, $\langle r_A \rangle = 1.23$ Å and $\sigma^2_{(A)} \sim 0.005$ Å^2 respectively. The $\langle r_A \rangle$ and $\sigma^2_{(A)}$ values for this set of samples were estimated using ionic radii of nine-fold coordination number [11].

Stoichiometric amounts of oxides and carbonates were dissolved, separately, in a solution of nitric acid and de-ionized water. After this, all metallic solutions were mixed together in an aqueous citric acid solution (in a molar ratio of 3:1 of metallic cations) which was heated up to ~ 50°C. This solution, to which ethylene glycol (4:6 molar ratio of the citric) was added, was then heated up to 70°C. The pH value was increased to about 5 by addition of ammonia. The resulting solution was turned to a gel by heating in temperatures of 90°C. Afterwards the gel was heat-treated to 200°C (2 h) at 1°C/min ratio and from 200°C up to 400°C (4 h) at 2°C/min. The resulting powder was ground and calcined in a temperature of 700°C for 12 h, reground and calcined again at 800°C for another period of 12 h. After that, powder was pelletized and sintered for 12 h at 1200°C in a flowing oxygen atmosphere.

The crystallographic structures were investigated by X-ray diffraction (XRD) using a Siemens-D5000 equipment. Magnetoresistance studies were performed in a Physical Properties Measurement System (Quantum Design), using the standard four probe method to measure the field- and temperature-dependent resistance of the sample $R(H,T)$. Measurements were taken between 100 and 360 K with applied fields up to 70 kOe on parallelepiped-shaped samples (all with almost similar dimensions, of the order of $1.0 \times 1.2 \times 4.0$ mm^3). Magnetization (M) measurements were performed in a SQUID magnetometer (Quantum Design). Measurements were carried out under fields up to 50 kOe, at temperatures from 2 K up to 350 K, and were taken either while warming the sample after cooling it in the absence of a field (ZFC), and while cooling in a field (FC).

T_C was determined as the temperature where dM/dT is minimum and T_{MS} as the maximum of the resistance versus temperature curve. The magnetoresistance was defined as $MR = [(R(0) - R(H))/R(0)] \times 100\%$, and the peak temperature of the magnetoresistance curve was labeled as T_{MR}. The compositions of the samples prepared, and their respective labels are: $La_{0.51}Gd_{0.16}\mathbf{Sr_{0.33}}MnO_3$ (LGS), $La_{0.53}Tb_{0.14}\mathbf{Sr_{0.33}}MnO_3$ (LTS), $La_{0.13}Pr_{0.54}\mathbf{Sr_{0.32}Ba_{0.01}}MnO_3$ (LPSB) and $La_{0.57}Ho_{0.10}\mathbf{Sr_{0.31}Ca_{0.02}}MnO_3$ (LHSC). All were prepared to have the following nominal values: $Mn^{4+} = 0.33$, $\langle r_A \rangle = 1.23$ Å and $\sigma^2_{(A)} \sim 0.005$ Å^2.

3. Results and discussion

As shown in Fig. 1, the X-ray diffraction patterns of all samples indicate that a single phase of the

perovskite-type structure was formed. No extra peaks were observed, indicating the absence of secondary phases. The inset of Fig. 1 reveals the presence of

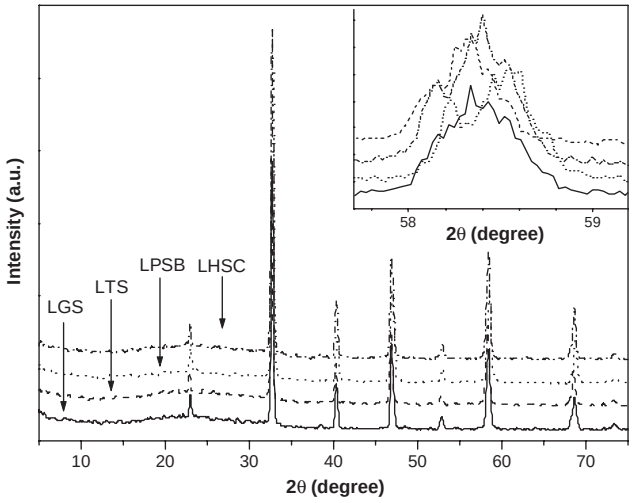

Fig. 1. X-ray diffraction pattern of the studied samples shown. Meaning of labels is given in Table 1.

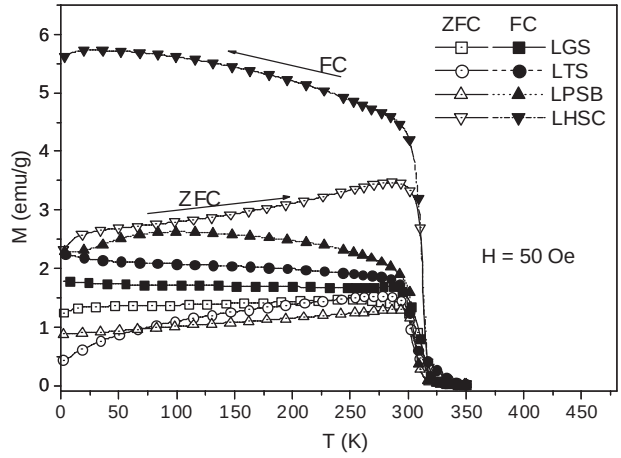

Fig. 2. Temperature dependence of magnetization for the studied samples under 50 Oe taken on warming after cooling the sample in zero-field (ZFC) and cooling runs in a field (FC) of 50 Oe.

double-peak structures for samples LPSB and LHSC, possibly indicating a slight difference in their structural symmetries. This could be possibly ascribed to the fact that these samples have up to four elements with different ionic radii in the *A*-site, being thus expected that different local distortions of lattice be formed, what could diminish the structural symmetry. Also noticeable is the absence of peak shifts from sample to sample, indicating no significant variation on the volume of the unit cell.

The temperature dependence of the magnetization of the studied compounds under an applied field of 50 Oe is shown in Fig. 2 (ZFC and FC procedures). The T_C values for all samples, collected in Table 1, are all very close to each other, within the temperature range 303–314 K. This suggests that the magnetic structure is probably preserved, indicating that the competition between antiferromagnetic (AFM) and ferromagnetic (FM) interactions are similar for all samples. According to de Gennes [3] the competition between superexchange (AFM) and double-exchange (FM) interactions define the magnetic structure, and can lead to a canted or helical spin structure. This might be indicative that at room temperature the DE interaction is roughly the same for all samples, and that this situation does not change as temperature decreases. Although ions in the *A*-site have different characteristics, no influence on the magnetic structure was observed, indicating that, close to room temperature, rare-earth ions are likely to be in the paramagnetic state in these compounds.

X-ray diffraction and magnetization measurements confirm those expected results at room temperature. From these results—position of peaks and T_C practically unchanged—one can also suggest that the oxygen content is essentially the same for all samples. Since, it has been shown that a decrease on the oxygen content leads to an increase of the volume and a decrease of magnetic transition temperatures [12].

We now focus on the influence of the rare-earth moments. The *RE* ions used in different compounds have different characteristics at low temperatures. In

Table 1
Nominal composition of the studied samples: $(R1_yR2_{1-y})^{+3}_{0.67}(M1_zM2_{1-z})^{+2}_{0.33}MnO_3$ ($R1$, $R2$ = La, Gd, Tb, Pr and Ho; $M1$, $M2$ = Ca, Sr, Ba) with $Mn^{4+} = 0.33$, $\langle r_A \rangle = 1.23$ Å and $\sigma^2_{(A)} \sim 0.005$ Å^2

Samples	Composition	T_C (K)	T_{MS} (K)	T_{MR} (K)	T_{Sh} (K)
LGS	$La_{0.51}Gd_{0.16}\mathbf{Sr_{0.33}}MnO_3$	312	234	296	303
LTS	$La_{0.53}Tb_{0.14}\mathbf{Sr_{0.33}}MnO_3$	303	230	295	291
LPSB	$La_{0.13}Pr_{0.54}\mathbf{Sr_{0.32}Ba_{0.01}}MnO_3$	306	244	304	300
LHSC	$La_{0.57}Ho_{0.10}\mathbf{Sr_{0.31}Ca_{0.02}}MnO_3$	314	250	306	308

Some distinctive temperatures are also shown for each sample.
T_C: magnetic transition temperature.
T_{MS}: metal-semiconductor transition temperature.
T_{MR}: peak temperature of MR curve.
T_{Sh}: temperature where R/R_{MAX} exhibits a change of slope.

fact, bulk Gd is ferromagnetic below $T_C = 293$ K, while bulk Tb is weakly ferromagnetic below $T_C = 231$ K. By its turn, bulk Ho is weakly ferromagnetic below $T_C = 20$ K, with a conical ordering of the moments. Between 20 K and $T_N = 132$ K, it has an AFM ordering, with helical structure. Bulk Pr orders antiferromagnetically at very low temperatures, with $T_N = 50$ mK. In general, bulk samples of the rare-earths order in complex magnetic structures at low temperatures, involving a great variety of anisotropic interactions [13,14].

Based on these observations, it is reasonable to expect that the interaction between Mn and rare-earth moments can result in the formation of complex magnetic structures, especially at low temperatures. This possibility has been discussed previously by Park et al. [15] for single crystals of some selected manganites. In Fig. 2 we observe that the magnetization (ZFC and FC) behavior below T_C is distinct for each composition of our samples. All samples present a decrease on the ZFC magnetization as the temperature decreases, indicating the appearance of a magnetic ordering which reduces the magnetization. This leads to the idea that an antiferromagnetic component of the exchange interaction is manifesting at these low temperatures. This can be due to the formation of a canted magnetic structure, as already suggested for other manganite compounds [16,17]. If one has a type of canted ordering, it is to be expected that a low applied field at some constant temperature, in this range below 20 K, should induce a transition to ferromagnetism. If the field required to induce the transition is small, it might be difficult to detect the related anomaly—an inflection point—in $M(H)$ curves as those displayed in Fig. 3. The temperature dependence of dM/dH (inset of Fig. 3), however, presents the indicative peak which reveals the occurrence of a field-induced magnetic transition from a canted state to a FM one [18].

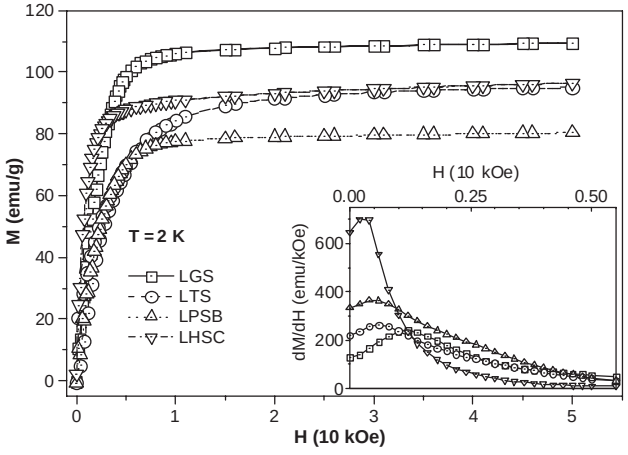

Fig. 3. Applied field dependence of magnetization for the studied samples at 2 K. Inset: dM/dH as a function of the applied field at 2 K.

In the low-temperature region of Fig. 2 (below $T \approx 50$ K) one can observe that, under a magnetic field of 50 Oe, the antiferromagnetic component is switched to ferromagnetic when samples LGS and LTS are field-cooled. However, for the LHSC sample one sees that the antiferromagnetic component persists for temperatures below 50 K, in spite of a tendency to switch to ferromagnetic ordering. For the LPSB sample, a marked decrease of magnetization is seen below 50 K, indicative that the dominant magnetic order is one that reduces M. These observations seem to suggest that the rare-earth moments in our compounds behave more or less as their corresponding bulk specimens, supporting our speculation that Gd and Tb order ferromagnetically, while for Ho and Pr the order is of the antiferromagnetic type. The following discussion elaborates more on this.

We address now the differences in magnetization magnitude for different samples. Of course one should expect that, if the above assumptions are correct, the rare-earth moments contribute for the saturation magnetization, M_S, except for the LPSB sample. This would thus suggest that M_S should be larger than the theoretical value, $M_{ST} = NgS_{ave}\mu_B$, calculated assuming full alignment of all Mn^{3+} and Mn^{4+} ions. In the expression, N is the number of Mn ions per volume unit, g is the gyromagnetic ratio ($g_{Mn} = 2$), μ_B is the Bohr magneton, and S_{ave} is the average spin of the constituents, namely $S = 2$ for Mn^{3+} and $S = 3/2$ for Mn^{4+}. For our compounds, with fully aligned Mn^{3+} (67%) and Mn^{4+} (33%), $M_{ST} \sim 90$ emu/g.

Fig. 3 depicts the magnetization versus applied field curve at 2 K for fields up to 50 kOe for all compounds. Values for the saturation magnetization are 109 emu/g for LGS, 95 emu/g for LHSC and LTS, and 80 emu/g for LPSB. These results reveal that, for samples LGS, LTS and LHSC, the presence of rare-earth moments contribute to increase M_S, suggesting that these ions are coupled ferromagnetically with the Mn magnetic structure. On the contrary, the LPSB sample, in spite of the higher content of substitutional rare-earth ions, has the lowest value of M_S, even smaller than the theoretical figure of 90 emu/g. This must be related to the presence of interactions depressing the magnetic moment of the sample, what might be supported by the fact, reported by Jensen and Mackintosh [14], that antiferromagnetism can be induced in Pr by an internal coupling due magnetic impurities, shifting T_N for higher temperatures. Thus, an antiferromagnetic coupling between Pr and Mn moments is plausible, leading to a substantial canting of the Mn magnetic structure and, consequently, decreasing M_S. The decrease of the FC magnetization observed (Fig. 2) for the LPSB sample below 50 K, is probably due to an antiferromagnetic alignment of Pr ions induced by field. A similar behavior seems to be present for the Ho-substituted sample.

Also in Fig. 3 one can observe different degrees of difficulty in promoting the magnetic alignment as the applied field is increased from 0 to 10 kOe. This can be better shown through the normalized curves M/M_S (Fig. 4). For the LGS, LPSB and LHSC samples, $M(H)$ quickly increases under applied fields lower than 10 kOe. However, for the LTS sample the process of magnetization is somewhat slower, which is contrary to that expected if Tb moments were simply ferromagnetically aligned with Mn moments. Thus, we must expand the discussion regarding this possible coupling between Mn and rare-earth moments, suggested by the experimental data. In a more complete analysis one has to consider that the position of the rare-earth ions are different from the ones they occupy in the corresponding bulk specimens. While the symmetry of our samples can be treated as cubic, bulk specimens of the rare-earths employed here as substitutionals have hexagonal symmetry. However, although the structural characteristics of the rare-earth bulks are similar, their magnetic properties differ considerably, mainly because the ordering of the rare-earth moments in the crystallographic planes are different. In the case of the samples studied here, magnetization data seem to indicate that the rare-earth moments in ground state are canted with respect to the Mn magnetic lattice. This is reflected by the data shown in Fig. 4, where the relative magnetization, normalized to one at saturation, highlights the contrasting differences experienced by each sample to have its moments aligned with the external field. For example, in the case of the LTS sample, we speculate that the canting angle between Mn and Tb is higher than the corresponding angle between the rare-earth and Mn for the others samples. This would also explain the behavior of the magnetization at low temperatures (Fig. 2). When submitted to a ZFC procedure, Mn moments align with the rare-earth moments at low temperatures and, when a field is applied, this configuration is maintained until thermal fluctuations are large enough to decouple the two sublattices which however will remain coupled only to the magnetic field. On the other hand, under a FC procedure, both Mn and rare-earth moments remain aligned along the applied field. From this reasoning one sees that the results of magnetization seem to be compatible with the existence of a magnetic interaction between Mn and rare-earth ions at low temperatures.

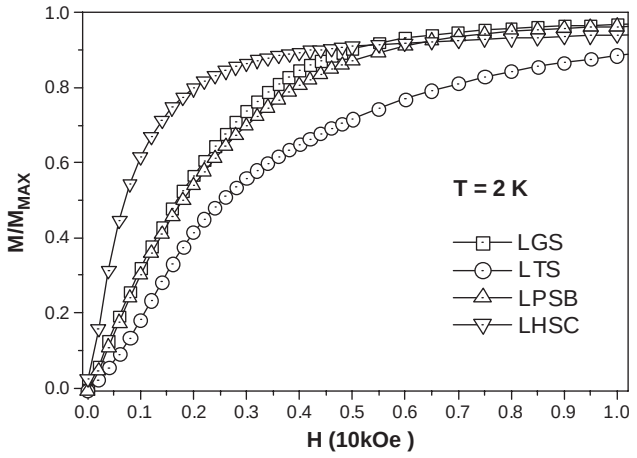

Fig. 4. Normalized magnetization as a function of the applied field at 2 K.

We turn now our discussion to the resistance versus temperature curves, taken with and without an applied field. In general terms, resistance curves should also reflect the magnetic behavior, and their overall characteristics can be compared to those revealed by magnetization curves. Measured in the absence of a magnetic field, a similar electrical behavior is expected for all samples. Under an applied field, however, resistance curves should differ at temperatures well below those of the magnetic transition region, while above this region these curves should be similar. In the transition region the resistance should mirror the magnetic behavior.

It is worth mentioning that the resistance values are approximately of the same order for all samples studied here. In order to compare the overall behavior of different specimens, we deal only with the normalized resistance, R/R_{MAX}. The temperature dependence of R/R_{MAX} measured in the absence of magnetic fields, for all prepared samples, is shown in Fig. 5. The curves almost overlap, and were shifted vertically for the sake of clarity. All curves exhibit a maximum at a temperature labeled T_{MS}, at which the sample undergoes a metal-to-semiconductor transition. For all samples, T_{MS} is found to occur between 230 and 250 K (Table 1) and, for each sample, this temperature is lower than the corresponding T_C. All curves exhibit a shoulder above T_{MS}, at which there is a sudden change of slope. In the temperature region where the shoulder appears, the experimental curves can be approximated by two straight lines. We have drawn such lines to emphasize the abrupt change of slope, occurring at T_{Sh}, indicated by arrows. Not surprisingly, this shoulder corresponds to the magnetic transition, as has been observed previously by other authors [19]. A simple inspection on Table 1 shows that this correspondence between T_C and T_{Sh} is reasonable. It is easily explained by the argument that electrical conductivity depends on the spin ordering. The inset of Fig. 5 shows the temperature derivative of R/R_{MAX}, to further demonstrate the change of slope discussed above.

The similarity of these curves confirms that the magnetic structure is preserved for all samples, since the transport mechanism depends on the Mn spin ordering [1]. This indicates clearly no influence of the rare-earth moments on the magnetic structure. Also, one is led to conclude that the crystallographic structures for all samples are quite similar, since a variation of the cell

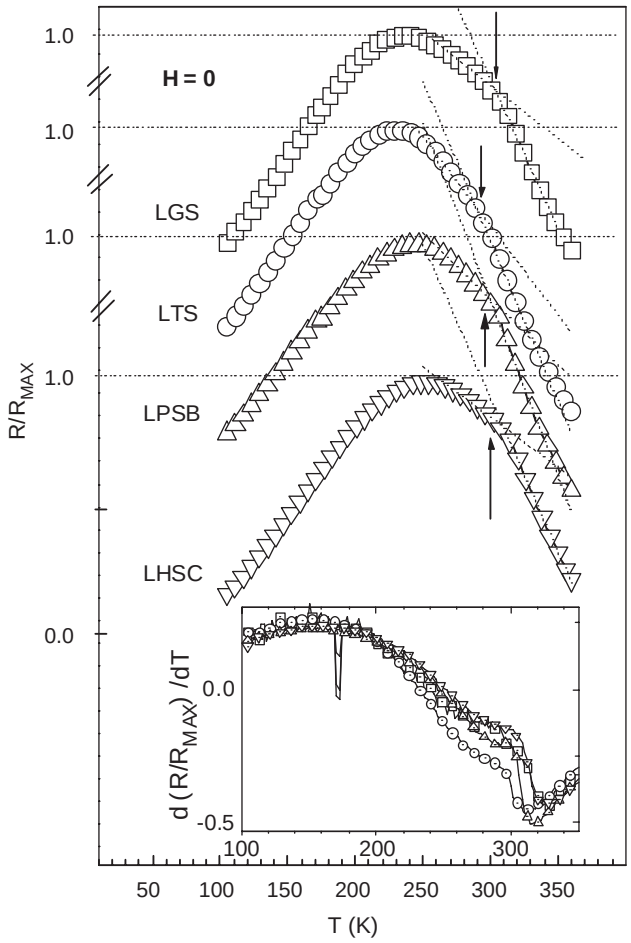

Fig. 5. Normalized resistance as a function of the temperature for the studied samples. For the sake of clarity, the curves were shifted vertically. Dashed straight lines emphasize the change of slope at the shoulder. Arrows indicate T_{Sh}. Inset: Temperature derivative of R/R_{MAX}, highlighting the change of slope.

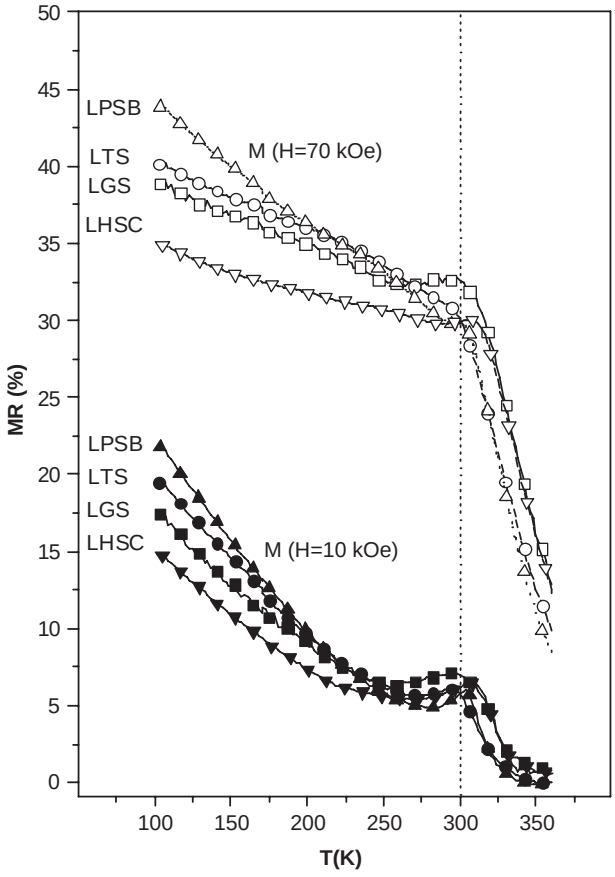

Fig. 6. Temperature dependence of the magnetoresistance, measured at 10 and 70 kOe.

volume would lead to a corresponding change on the Mn–O–Mn bond angle and, thus, on the magnetotransport response. For example, in $La_{0.67}Ca_{0.33}MnO_3$, when La is substituted by Y to form $La_{0.60}Y_{0.07}Ca_{0.33}MnO_3$ [20], the lattice parameters diminish by some 0.2%, while T_{MS} and T_C are shifted down by 90 K. For that system, on T_C the shift represents a change of 0.34%, whereas the corresponding percentage is smaller than 0.04% in the present case.

Magnetoresistance versus temperature curves when the samples studied were submitted to applied fields of 10 and 70 kOe, are presented in Fig. 6. Each of them exhibits a local maximum around T_C. Below 250 K, the MR (both for 10 and 70 kOe) increases monotonously as the temperature decreases. If only Mn and its magnetic structure were affected, then we should expect similar slopes ($dMR = \Delta MR/\Delta T$) for all curves. Contrarily, if the applied field induces ordering of the rare-earth moments, a consequence could be a non-negligible interaction between Mn and rare-earth moments, affecting the Mn magnetic structure responsible by the DE mechanism. The different slopes observed in Fig. 6 below 250 K for all samples clearly indicate that the magnetic response on the spin structure under an applied field is different from sample to sample as the temperature decreases. Thus, the rare-earth contribution seems to be a necessary ingredient to explain these results. Now, we also observe that the slopes of the MR curves at 70 kOe associated to samples LTS and LGS are identical, below 225 K, what is possibly related to the ferromagnetic behavior of Tb and Gd moments, as suggested earlier in this analysis. This observation is consistent with the fact that, at high fields, both Mn and rare-earth moments are aligned along the external field and, thus, the interaction between them should be similar in both samples. However, the slopes of samples LHSC and LPSB are very different. This might be attributed to a more complex magnetic behavior, as also suggested earlier. In the transition region (280–315 K), the values of the MR peak and of the corresponding temperature where it takes place, T_{MR}, differ from one specimen to another, what is expected, since position, size and shape of the MR peak are strongly correlated to the magnetic transition. Above 315 K the slopes of all MR curves are very similar, indicating that, as expected,

the transport mechanism is the same for all samples in the paramagnetic phase.

In order to verify the magnetic state of rare-earth ions in our samples, we have measured the MR versus applied field at 300 K, a temperature for which the rare-earth ions are paramagnetic when in bulk specimens, but all the samples studied here are ferromagnetic ($T_C > 300$ K, see Table 1). Now, if the rare-earth ions are found in the paramagnetic state, they should have a similar behavior under an applied field and, consequently, should cause similar effects on the Mn magnetic structure. The magnetoresistance measurements, shown in Fig. 7, corroborate the expected behavior, revealing an approximately linear increase of MR with the applied field, being the MR values for different samples very close to each other, within measured field range, from 0 up to 70 kOe. This indicates that the magnetic structure responds similarly under an applied magnetic field and, consequently, that the mechanisms of electrical conduction are similar for all samples studied. In short, these results obtained from transport measurements corroborate those obtained from magnetization experiments.

In summary, we have reported the results of magnetic and electrical measurements of compounds $(R1_yR2_{1-y})^{+3}_{0.67}(M1_zM2_{1-z})^{+2}_{0.33}MnO_3$ ($R1$, $R2$ = La, Gd, Pr, Ho, Tb, Y; $M1$, $M2$ = Ca, Sr). It is clear that our results of transport, magnetization and XRD measurements show that magnetic and crystallographic structures are quite similar for all compounds at room temperatures, in spite the disparity of A-site cations due to the difference in ionic radius. Results were discussed on the basis of the coupling between Mn and rare-earth moments, taking as fixed the parameters Mn^{3+}/Mn^{4+} ratio and crystal structure.

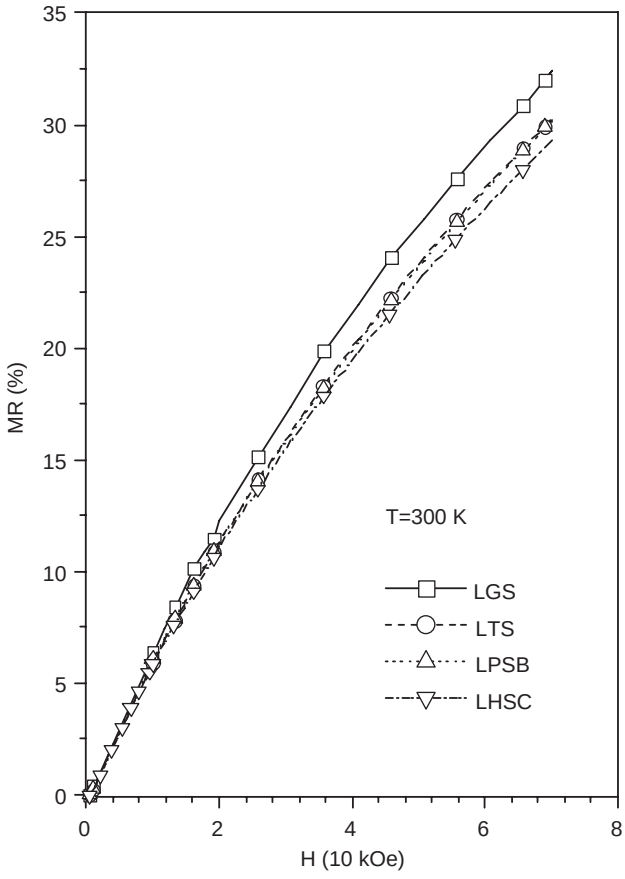

Fig. 7. Applied field dependence of the magnetoresistance, taken at 300 K for applied fields from 0 up to 70 kOe.

4. Conclusion

We have shown that, maintaining constant structural parameters (Mn^{3+}/Mn^{4+}, $\langle r_A \rangle$ and σ^2) and the preparation conditions, we were able to obtain samples with similar structural, magnetic and electric properties. The magnetization measurements indicate that the rare-earth ions in our samples have similar behavior as compared to those of the respective bulks. Therefore, one might expect that complex magnetic structures will be formed at low temperatures. We have also observed that T_C is similar for all studied samples, indicating that the specific magnetic characteristics introduced by different rare-earth ions are irrelevant at high temperatures. However, at low temperatures an anomalous behavior of the magnetization shows evidence of magnetic coupling between of Mn and rare-earth moments, as discussed previously by others.

Acknowledgments

The authors acknowledge partial support from Brazilian agencies Fundação de Amparo à Pesquisa do Estado de São Paulo (FAPESP) and Conselho Nacional de Desenvolvimento Científico e Tecnológico (CNPq).

References

[1] C. Zener, Phys. Rev. 81 (1951) 440;
C. Zener, Phys. Rev. 82 (1951) 403.
[2] C. Mitra, P. Raychaudhuri, S.K. Dhar, A.K. Nigam, R. Pinto, S.M. Pattalwar, J. Magn. Magn. Mater. 192 (1999) 130.
[3] P.G. Gennes, Phys. Rev. 118 (1960) 141.
[4] A. Maignan, Ch. Simon, V. Caignaert, B. Raveau, Phys. B 99 (1996) 305.
[5] F. Damay, C. Martin, A. Maignan, B. Raveau, J. Appl. Phys. 82 (1997) 6181.
[6] L.M. Rodriguez-Martinez, J.P. Attfield, Phys. Rev. B 54 (1996) R15622.
[7] J.P. Attfield, Chem. Mater. 10 (1998) 3239.
[8] B. Raveau, A. Maignan, C. Martin, M. Hervieu, Chem. Mater. 10 (1998) 2641.
[9] P. Schiffer, A.P. Ramirez, W. Bao, S.-W. Cheong, Phys. Rev. Lett. 75 (1995) 3336.

[10] M.P. Pechini, US patent Nr 3300 (1967) 679;
M. Kakihana, J. Sol–Gel Sci. Technol. 6 (1996) 7.
[11] R.D. Shannon, Acta Crystallogr. A 32 (1976) 751.
[12] H.L. Ju, J. Gopalakrishnam, J.L. Peng, G.C. Qi Li, T. Xiong, R.L. Venkatesan, Greene, Phys. Rev. B 51 (1995) 6143.
[13] E. Schreire, M. Ekstrom, O. Hartmann, R. Wappling, G.M. Kalvius, F.J. Burghart, S. Henneberger, A. Marelius, A. Kratzer, Physica B 289 (2000) 240.
[14] J. Jensen, A.R. Mackintosh, Rare Earth Magnetism: Structures and Excitations, Oxford University Press, Oxford, 1991.
[15] J.-G. Park, M.S. Kim, H.-C. Ri, K.H. Kim, T.W. Noh, S.-W. Cheong, Phys. Rev. B 60 (1999) 14408.
[16] J. Park, M.S. Kim, J.-G. Park, I.P. Swainson, H.-C. Ri, H.J. Lee, K.H. Kim, T.W. Noh, S.-W. Cheong, C. Lee, J. Korean Phys, Soc. 36 (2000) 412.
[17] P. Raychaudhuri, T.K. Nath, P. Sinha, C. Mitra, A.K. Nigam, S.K. Dhar, R. Pinto, J. Phys.: Condens. Matter 9 (1997) 10919.
[18] Z.B. Guo, H. Huang, W.P. Ding, Y.W. Du, Phys. Rev. B 56 (1997) 10789.
[19] A.K. Pradhan, B.K. Roul, J.G. Wen, Z.F. Ren, M. Muralidhar, P. Dutta, D.R. Sahu, S. Mohanty, P.K. Patro, Appl. Phys. Lett. 76 (2000) 763.
[20] S. Jin, H.M. O'Bryan, T.H. Tiefel, M. McComacK, W.W. Rhodes, Appl. Phys. Lett. 66 (1995) 382.